JOURNAL OF MATERIALS SCIENCE 9 (1974) 1183–1188

The structure of splat-cooled Fe–20% Cr–25% Ni austenitic steel

J. V. WOOD, R. W. K. HONEYCOMBE
Department of Metallurgy and Materials Science, University of Cambridge, Cambridge, UK

A controlled atmosphere splat quenching gun has been used to produce splats of Fe–20% Cr–25% Ni. Three types of structure were observed by thin foil electron microscopy, namely high-angle cellular, low-angle cellular, and linear arrays of dislocation loops, which were determined primarily by the heat transfer conditions. In the thin, most rapidly cooled areas (lift-off regions) high-angle cellular structures were observed which were largely free of defects. As the cooling rate decreases there was a greater tendency for low-angle cellular structures to form, but at intermediate cooling rates bands of dislocation loops were observed. These are explained in terms of solute segregation and vacancy coalescence along $\langle 100 \rangle_{\gamma}$ directions in the austenite.

1. Introduction

Despite the voluminous literature on splat cooling (see, for example, the recent bibliography of Jones and Suryanarayana [1]), there have been relatively few specific investigations into the solidification structure of rapidly cooled alloys. The present work describes the as-cast structure in a splat-quenched austenitic chromium nickel steel. This steel (Fe–20% Cr–25% Ni) was chosen because it does not undergo a solid state phase transformation during quenching, but provides a single phase fcc solid solution, which has received detailed structural studies after more conventional heat-treatments. Less highly alloyed austenitic steels (e.g. Fe–18% Cr–10% Ni) form, on splat quenching, metastable phases which complicate the study of the as-quenched state, so these compositions are best left for future studies.

2. Experimental techniques

The "gun technique" of Duwez and Willens [2] affords the highest cooling rate in quenching from the liquid state. Iron-base alloys are difficult to splat for three reasons: (i) high melting points; (ii) oxidation of metal spray; (iii) possible metal-crucible reactions. These points were realized by Ruhl and Cohen [3] who consequently used a controlled atmosphere gun.

In the present work, a modified controlled atmosphere gun was developed [4] which allows alloys with melting points up to 1700°C to be splat cooled. Heat energy was supplied by means of an r.f. source, melting a sample of about 0.2 g. This was held in an alumina crucible with an orifice diameter of 0.4 mm. The plastic (melinex) diaphragm ruptured between 3.0 to 4.0 MN m^{-2} depending on the film thickness. Variation of the rupture pressure did not affect the resulting microstructures. The molten droplet was ejected onto a curved copper substrate roughened by 400 grade emery paper in two directions. The substrate was placed 10 cm from the orifice and was water cooled throughout each experiment.

Two argon arc melts of 20% Cr–25% Ni steel were made, differing only in the amount of dissolved oxygen in the iron, to check the effect of dissolved gases on the structure of the splats. The first alloy contained 400 ppm dissolved oxygen, the second < 20 ppm dissolved oxygen. After melting, the alloys were homogenized, hot-rolled and swaged to 2.5 mm diameter rod. Residual oxide was removed from the surface by electro-polishing. Samples were cut from this rod for insertion in the quenching apparatus.

After the chamber enclosing the gun had been pumped down to a vacuum of 10^{-5} Torr, a partial pressure of 550 Torr high purity argon was introduced. The alumina crucible was enveloped by a block of high purity graphite which acted as a getterer to remove any residual traces of oxygen in the closed system. The small orifice diameter and the relatively high surface tension of this alloy led to the molten stream breaking up and forming a number of small splats on the copper substrate.

The phase identity was checked by X-ray diffraction on all splats. In every case austenite was the only phase present, though an accurate lattice parameter could not be assigned due to the broadness of the lines.

Foils were directly observed in transmission in a Jeol 200 kV electron microscope. Some specimens were ion-beam thinned to show the internal structure of slightly thicker regions. The fineness of the microstructure and the physical size of each splat limits the use of optical microscopy, so scanning electron microscopy was used as an alternative.

3. Results and discussion

3.1. Large scale structure of splats

As-quenched, the alloy solidifies primarily in a cellular form, without the formation of secondary dendrite arms. The structure is illustrated in Fig. 1a (optical micrograph) and Fig. 1b (scanning electron micrograph). At more conventional cooling rates achieved in casting, Cr–Ni austenitic steels solidify in a dendritic fashion and are heavily cored with respect to Cr and Ni [5]. The present alloy behaved in this way when chill cast in a copper water-cooled mould.

Recent work on splat-cooled Fe–25% Ni [6] using the piston and anvil technique, has shown that there is appreciable Ni microsegregation if the droplet is highly undercooled. Kattamis *et al.* find no evidence of Ni segregation in superheated droplets, but the resolution of the microprobe is not sufficient to examine precisely such fine structures.

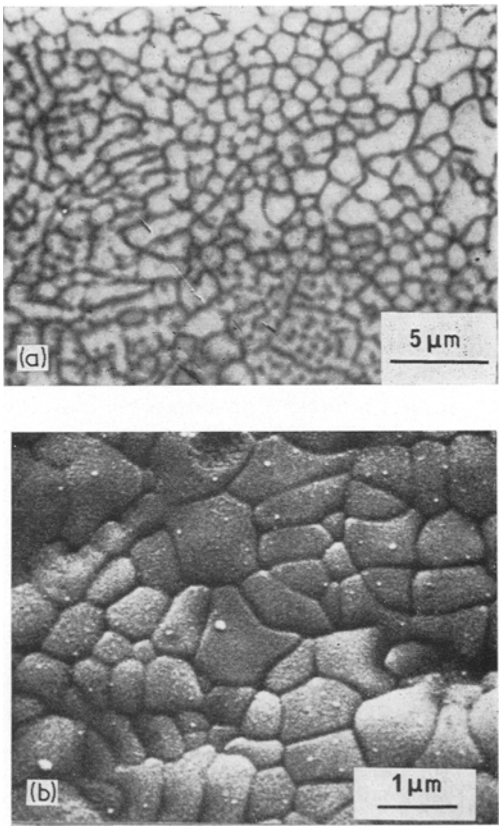

Figure 1 (a) Optical micrograph, (b) scanning electron micrograph (unetched) of "as-splatted" 20% Cr–25% Ni–Fe.

3.2. Transmission electron microscopy – typical structures

Using a 200 kV electron microscope, thin areas were observed both at the edge and within the splats. Three main types of structure were observed: (1) normal cellular (high-angle); (2) low-angle cellular; (3) linear loop array. These are illustrated in Fig. 2.

3.2.1. Normal cellular structures

The typical cellular structure is seen in Fig. 2a and b, showing cells growing in the plane of the foil (Fig. 2a) and normal to the plane of the foil (Fig. 2b). The latter structure would be expected if the heat is removed directly into the copper substrate, nevertheless it is not often seen on splats which have not been subjected to further thinning. Scanning electron microscopy of splatted surfaces indicate that a high proportion of the splat exhibits this type of cellular structure: however, in as-splatted foils, cells growing in the plane of the foil predominate. If the specimens are then further thinned by the ion-beam thinning technique, the cellular structure normal to the plane of the foil is much more frequently observed.

Scanning electron microscopic examination of the undersides of the splats (Fig. 3) indicated that while large areas replicated the copper surface, there were small regions which were comparatively smooth. These are interpreted as "lift-off" areas, which could arise from several causes: (i) gas entrapment underneath the solidifying splat; (ii) thermal contraction during solidification; (iii) cavitation as a result of the

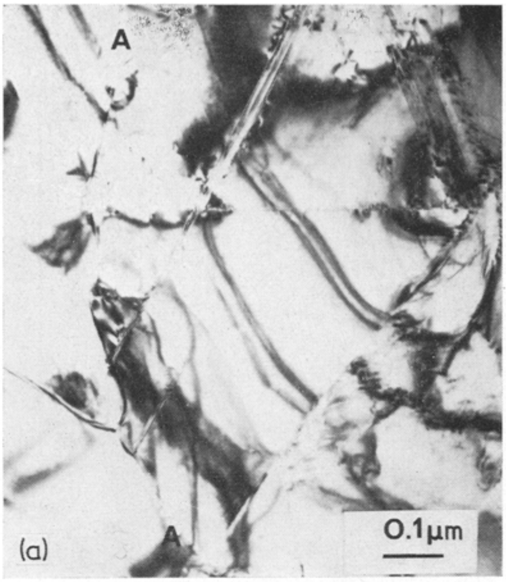

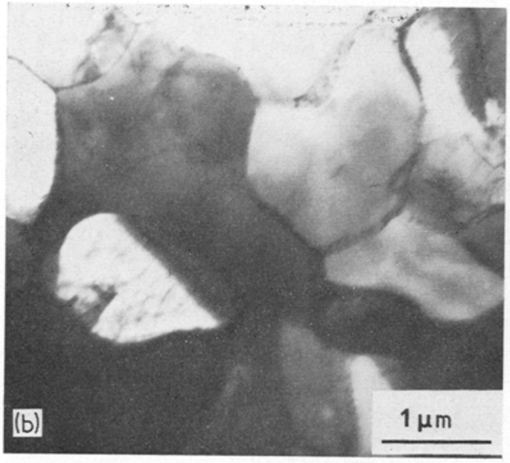

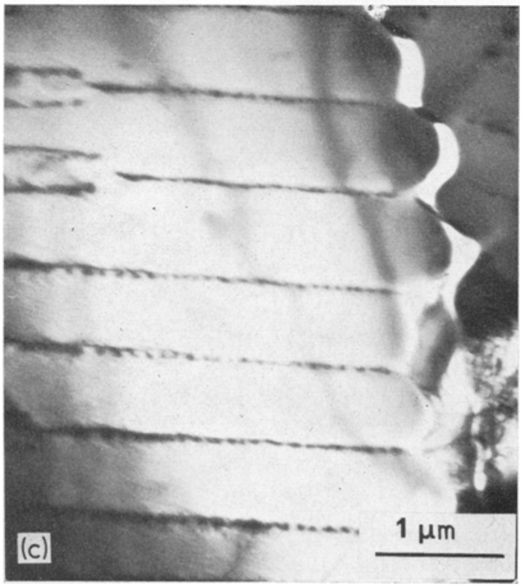

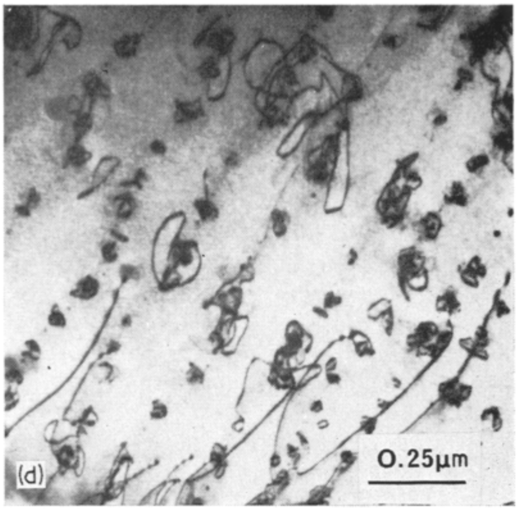

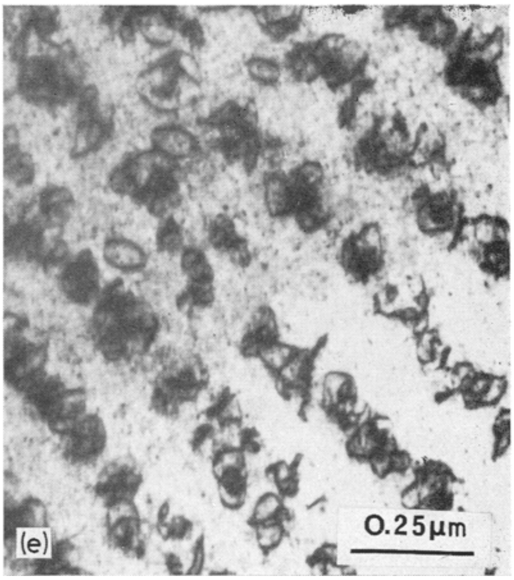

Figure 2 Typical structures of splats of 20% Cr–25% Ni–Fe as observed by transmission electron microscopy. (a) High-angle cells growing in plane of foil. (b) High-angle cells growing perpendicular to foil (ion-beam thinned). (c) Low-angle cells. (d) Linear dislocation loop arrays. (e) Tangled dislocation arrays.

shearing of the solidifying droplet over surface asperities on the substrate. Whatever the real explanation, the phenomenon is very common in the present experimental arrangement, and scanning electron microscopy has shown that these "lift-off" areas often exhibit cellular structures growing in the plane of the foil (Fig. 4), implying that the heat loss in the immediate vicinity is also in the plane of the foil. As the thinnest areas show cellular structure of this type it is assumed, therefore, that they are associated with "lift-off" areas.

Applying the heat transfer criteria used by Ruhl [7] it can be shown that the rate of cooling in such areas is not greatly different from the contact areas, provided that the "lift-off" areas are not larger than 20 μm in diameter. With larger areas of "lift off", the rate of heat extraction is significantly slower, with the result that the cellular structure breaks down to give branching and segregation within each grain (Fig. 5).

The cellular structure in the thinnest areas of as-splatted specimens are generally characterless with a low dislocation density. Such areas are comprised of parallel sided "fingers" abutting on a common boundary (Fig. 2a), the orientation difference across the longitudinal boundary of the cells being random.

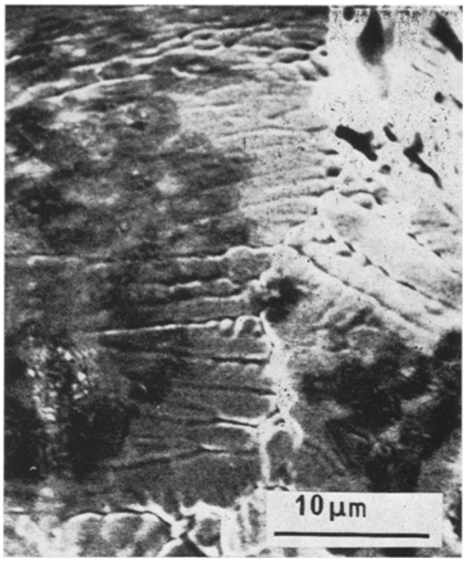

Figure 4 Scanning electron microscope micrograph of "lift off" area showing cell growth in the plane of foil.

3.2.2. Low-angle cellular structures

In some areas (Fig. 2c), randomly orientated cells are replaced by exactly parallel sided boundaries lying in the ⟨100⟩ direction. The angular mismatch across such boundaries is small. Unlike the random orientated cells which meet along a straight boundary, these low angle cells have a perturbed growth front, indicating that the cooling rate has been slower in these regions.

3.2.3. Structures with linear loop arrays

Proceeding from the thin featureless regions to slightly thicker areas, but still thin enough to observe, the "fingers" are replaced by rather larger grains. Within these grains bands of defects occur (Fig. 2d) which can be resolved as bands of dislocation loops, most of which are tangled (Fig. 2e). The bands are in $\langle 100 \rangle_\gamma$ directions, and on analysis the loops were found to possess a vector $\boldsymbol{b} = (a/2)\langle 110 \rangle$. Analysis of

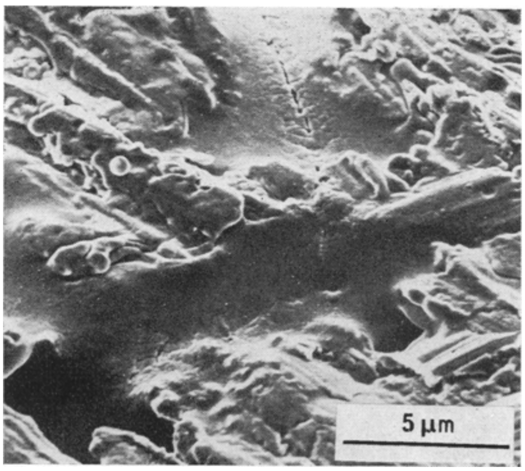

Figure 3 Scanning electron micrograph of underside of splat showing "lift off" areas.

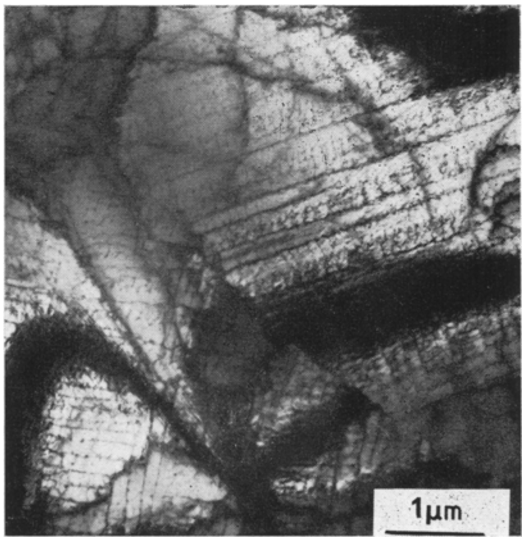

Figure 5 Large unthinned area of foil observed by transmission electron microscopy, showing branching and segregation.

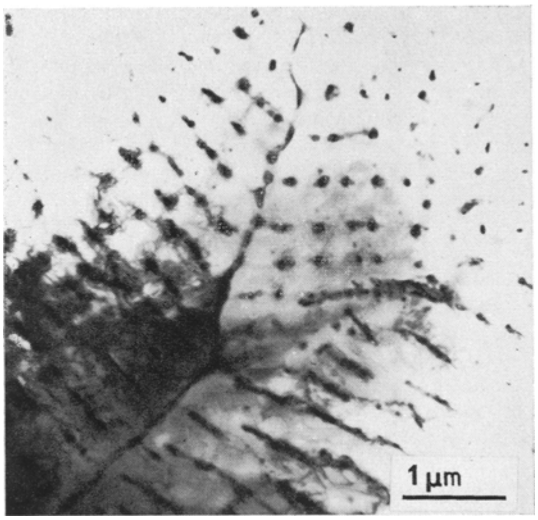

Figure 6 Ion-beam thinned foil, showing spheroidization of solute rods (transmission electron micrograph).

those loops which could be examined in detail showed that they were of the vacancy coalescence type.

Tiller has postulated [8] that dislocation loops can be formed during freezing of an alloy by at least three mechanisms: (i) stresses set up as a result of constitutional segregation; (ii) condensation of vacancies from the melt; (iii) loops punched out by small particles or voids. There is some evidence that segregation takes place along ⟨100⟩ directions during the solidification of Ni–Cr austenitic steels [5, 6]. In the present work similar evidence was obtained, for example in Fig. 6. According to Nichols and Mullins [9], long rods rich in solute will tend to spheroidize; this would give the structure illustrated in Fig. 6. Using the concept of a solute-rich rod entrapped during solidification, we find that the stresses arising from differential thermal contraction could generate the observed number of loops if it is assumed there is a difference of 1.5×10^{-6} change in length per unit micron length over the whole temperature range from the melting point to room temperature. That solute segregation is to some degree involved in loop generation was shown by splatting pure nickel in which no loops were observed. On the other hand, detailed analysis of the loop bands in the 20/25 alloy using an analytical electron microscope (EMMA 4) failed to resolve any significant segregation.

Previous theoretical work [10] has shown that loops can form when vacancies form directly from the melt, in contrast to Jaffrey and Chadwick [11] who stress the necessity for a nucleating particle or gas bubble. The work of Thomas and Willens [12] showed that randomly distributed loops were produced in splat-quenched aluminium. Their work does not, however, help to explain the banded structures of loops observed in the present investigation.

Under normal solidification conditions, dislocation sub-boundaries are a familiar characteristic of slightly impure metals. The dislocation array size m has been determined theoretically by Frank [13] as:

$$m^2 = \frac{D_V \, . \, k \, . \, T^2}{V_m \, . \, v \, . \, G_S}$$

where D_V is the diffusion coefficient of vacancies, V_m is the specific volume, v is the growth velocity, G_S is the temperature gradient in the solid. Inserting reasonable values for the present experimental conditions (based on values for splat quenching of aluminium [14]) a value of 10^{-6} cm is obtained for the dislocation array size, which compares with the experimentally observed values around 3×10^{-5} cm.

In metals frozen at normal rates, solute atom impurities become associated with the dislocation arrays [15]. There is some evidence that solute atoms are also associated with the dislocation networks in splat-cooled austenitic steel. It is thus proposed that the bands of dislocation loops arise from the direct entrapment of vacancy aggregation from the melt, leading to dislocations which form linear arrays during cooling, and become associated with progressive solute segregation typical of most solidification processes.

The usage of high purity materials and the fact that dissolved oxygen content does not affect the microstructure means that the third method of loop formation can be ignored in the present work.

4. Conclusions

1. Fe-20% Cr-25% Ni does not undergo a metastable phase change during splat quenching.

2. Three distinct structures are observed and can be related to the local cooling conditions. Between the segregated and homogeneous cell structures there is an intermediate structure characterized by long parallel bands of dislocation loops lying in the ⟨100⟩ direction.

3. These loops have a Burgers vector of

$(a/2)$ $\langle 110 \rangle$ and are of a vacancy coalescence type.

4. This phenomenon is associated with both vacancy condensation and solute atoms.

5. Pure nickel grows in a similar cellular fashion but does not show linear defect bands, though random defects are observed.

6. Thin areas must be correlated with the local cooling conditions as they are not necessarily the areas that have undergone the fastest cooling cycle.

Acknowledgements

We are grateful to Dr G. W. Lorimer for carrying out the microanalysis using an EMMA microscope, and to Dr P. Beaven for guidance in the analysis of dislocation loops. One of us (J.V.W.) thanks the Science Research Council for provision of a Studentship. We also gratefully acknowledge support from the Science Research Council for the construction of the splat quenching apparatus.

References

1. H. JONES and C. SURYANARAYANA, *J. Mater. Sci.* **8** (1973) 705.
2. P. DUWEZ and R. H. WILLENS, *Trans. Met. Soc. AIME* **227** (1963) 362.
3. R. C. RUHL and M. COHEN, *ibid* **245** (1969) 241.
4. M. G. SCOTT and J. V. WOOD, University of Cambridge, unpublished work.
5. H. FREDRIKSSON, *Met. Trans.* **3** (1972) 2989.
6. T. Z. KATTAMIS, W. F. BROWER and R. MEHRABIAN, *J. Crystal Growth* **19** (1973) 229.
7. R. C. RUHL, *Mat. Sci. Eng.* **1** (1966) 313.
8. W. A. TILLER, "Physical Metallurgy" 2nd Edn (edited by R. W. Cahn) (North Holland, Amsterdam, 1970) p. 442.
9. F. A. NICHOLS and W. W. MULLINS, *Trans. Met. Soc. AIME* **233** (1965) 1840.
10. G. F. BOLLING and D. FAINSTEIN, *Phil. Mag.* **25** (1972) 45.
11. D. JAFFREY and G. A. CHADWICK, *ibid* **18** (1968) 573.
12. G. THOMAS and R. H. WILLENS, *Acta Met.* **12** (1964) 191.
13. F. C. FRANK, "Deformation and Flow in Solids" Madrid Conference (Springer-Verlag, Berlin, 1956) p. 73.
14. P. PREDRECKI, A. W. MULLENDORE and N. J. GRANT, *Trans. Met. Soc. AIME* **233** (1965) 1581.
15. H. A. ATWATER and B. CHAMBERS, *J. Chem. Phys.* **35** (1957) 208.

Received 25 February and accepted 4 March 1974.